

Search for the decay $B^0 \rightarrow K^{*0} \tau^+ \tau^-$ at the Belle experiment

T. V. Dong,¹⁰ T. Luo,¹⁰ I. Adachi,^{16,12} H. Aihara,⁸⁵ D. M. Asner,³ H. Atmacan,⁷ V. Aulchenko,^{4,64} T. Aushev,¹⁸ R. Ayad,⁹² V. Babu,⁸ S. Bahinipati,²² P. Behera,²⁵ K. Belous,²⁹ F. Bernlochner,² M. Bessner,¹⁵ B. Bhuyan,²³ T. Bilka,⁵ J. Biswal,³⁴ A. Bobrov,^{4,64} A. Bozek,⁶¹ M. Bračko,^{49,34} P. Branchini,³¹ T. E. Browder,¹⁵ A. Budano,³¹ M. Campajola,^{30,56} D. Červenkov,⁵ M.-C. Chang,⁹ P. Chang,⁶⁰ A. Chen,⁵⁸ B. G. Cheon,¹⁴ K. Chilikin,⁴⁴ H. E. Cho,¹⁴ K. Cho,³⁹ S.-J. Cho,⁹¹ S.-K. Choi,¹³ Y. Choi,⁷⁸ S. Choudhury,²⁴ D. Cinabro,⁸⁹ S. Cunliffe,⁸ T. Czank,³⁶ S. Das,⁴⁸ G. De Nardo,^{30,56} G. De Pietro,³¹ R. Dhamija,²⁴ F. Di Capua,^{30,56} J. Dingfelder,² Z. Doležal,⁵ S. Dubey,¹⁵ D. Epifanov,^{4,64} T. Ferber,⁸ D. Ferlewicz,⁵¹ B. G. Fulsom,⁶⁶ R. Garg,⁶⁷ V. Gaur,⁸⁸ N. Gabyshev,^{4,64} A. Garmash,^{4,64} A. Giri,²⁴ P. Goldenzweig,³⁵ E. Graziani,³¹ T. Gu,⁶⁹ K. Gudkova,^{4,64} T. Hara,^{16,12} O. Hartbrich,¹⁵ K. Hayasaka,⁶³ M. Hernandez Villanueva,⁸ W.-S. Hou,⁶⁰ C.-L. Hsu,⁷⁹ K. Inami,⁵⁵ G. Inguglia,²⁸ A. Ishikawa,^{16,12} R. Itoh,^{16,12} M. Iwasaki,⁶⁵ W. W. Jacobs,²⁶ E.-J. Jang,¹³ S. Jia,¹⁰ Y. Jin,⁸⁵ K. K. Joo,⁶ J. Kahn,³⁵ K. H. Kang,⁴² H. Kichimi,¹⁶ C. Kiesling,⁵⁰ C. H. Kim,¹⁴ D. Y. Kim,⁷⁷ S. H. Kim,⁷⁵ Y.-K. Kim,⁹¹ T. D. Kimmel,⁸⁸ P. Kodyš,⁵ T. Konno,³⁸ A. Korobov,^{4,64} S. Korpar,^{49,34} E. Kovalenko,^{4,64} P. Križan,^{45,34} R. Kroeger,⁵² P. Krokovny,^{4,64} T. Kuhr,⁴⁶ R. Kulasiri,³⁷ M. Kumar,⁴⁸ R. Kumar,⁷⁰ K. Kumara,⁸⁹ A. Kuzmin,^{4,64} Y.-J. Kwon,⁹¹ M. Laurenza,^{31,73} S. C. Lee,⁴² J. Li,⁴² L. K. Li,⁷ Y. B. Li,⁶⁸ L. Li Gioi,⁵⁰ J. Libby,²⁵ K. Lieret,⁴⁶ D. Liventsev,^{89,16} C. MacQueen,⁵¹ M. Masuda,^{84,71} T. Matsuda,⁵³ D. Matvienko,^{4,64,44} M. Merola,^{30,56} F. Metzner,³⁵ K. Miyabayashi,⁵⁷ R. Mizuk,^{44,18} G. B. Mohanty,⁸⁰ M. Nakao,^{16,12} A. Natochii,¹⁵ L. Nayak,²⁴ M. Niiyama,⁴¹ N. K. Nisar,³ S. Nishida,^{16,12} K. Nishimura,¹⁵ S. Ogawa,⁸² H. Ono,^{62,63} Y. Onuki,⁸⁵ P. Oskin,⁴⁴ P. Pakhlov,^{44,54} G. Pakhlova,^{18,44} S. Pardi,³⁰ H. Park,⁴² S.-H. Park,¹⁶ S. Patra,²¹ S. Paul,^{81,50} T. K. Pedlar,⁴⁷ R. Pestotnik,³⁴ L. E. Pilonen,⁸⁸ T. Podobnik,^{45,34} V. Popov,¹⁸ E. Prencipe,¹⁹ M. T. Prim,² A. Rostomyan,⁸ N. Rout,²⁵ G. Russo,⁵⁶ D. Sahoo,⁸⁰ S. Sandilya,²⁴ A. Sangal,⁷ L. Santelj,^{45,34} T. Sanuki,⁸³ V. Savinov,⁶⁹ G. Schnell,^{1,20} J. Schueler,¹⁵ C. Schwanda,²⁸ Y. Seino,⁶³ K. Senyo,⁹⁰ M. E. Sevier,⁵¹ M. Shapkin,²⁹ C. Sharma,⁴⁸ J.-G. Shiu,⁶⁰ F. Simon,⁵⁰ E. Solovieva,⁴⁴ M. Starič,³⁴ M. Sumihama,¹¹ K. Sumisawa,^{16,12} T. Sumiyoshi,⁸⁷ M. Takizawa,^{76,17,72} U. Tamponi,³² K. Tanida,³³ F. Tenchini,⁸ K. Trabelsi,⁴³ M. Uchida,⁸⁶ Y. Unno,¹⁴ S. Uno,^{16,12} R. Van Tonder,² G. Varner,¹⁵ K. E. Varvell,⁷⁹ E. Waheed,¹⁶ C. H. Wang,⁵⁹ E. Wang,⁶⁹ P. Wang,²⁷ M. Watanabe,⁶³ S. Watanuki,⁴³ O. Werbycka,⁶¹ E. Won,⁴⁰ B. D. Yabsley,⁷⁹ W. Yan,⁷⁴ S. B. Yang,⁴⁰ H. Ye,⁸ J. H. Yin,⁴⁰ Z. P. Zhang,⁷⁴ V. Zhilich,^{4,64} and V. Zhukova⁴⁴

(The Belle Collaboration)

¹Department of Physics, University of the Basque Country UPV/EHU, 48080 Bilbao, Spain²University of Bonn, 53115 Bonn, Germany³Brookhaven National Laboratory, Upton, New York 11973, USA⁴Budker Institute of Nuclear Physics SB RAS, Novosibirsk 630090, Russia⁵Faculty of Mathematics and Physics, Charles University, 121 16 Prague, Czech Republic⁶Chonnam National University, Gwangju 61186, South Korea⁷University of Cincinnati, Cincinnati, Ohio 45221, USA⁸Deutsches Elektronen-Synchrotron, 22607 Hamburg, Germany⁹Department of Physics, Fu Jen Catholic University, Taipei 24205, Taiwan¹⁰Key Laboratory of Nuclear Physics and Ion-beam Application (MOE) and Institute of Modern Physics, Fudan University, Shanghai 200443, China¹¹Gifu University, Gifu 501-1193, Japan¹²SOKENDAI (The Graduate University for Advanced Studies), Hayama 240-0193, Japan¹³Gyeongsang National University, Jinju 52828, South Korea¹⁴Department of Physics and Institute of Natural Sciences, Hanyang University, Seoul 04763, South Korea¹⁵University of Hawaii, Honolulu, Hawaii 96822, USA¹⁶High Energy Accelerator Research Organization (KEK), Tsukuba 305-0801, Japan¹⁷J-PARC Branch, KEK Theory Center, High Energy Accelerator Research Organization (KEK), Tsukuba 305-0801, Japan¹⁸National Research University Higher School of Economics, Moscow 101000, Russia¹⁹Forschungszentrum Jülich, 52425 Jülich, Germany²⁰IKERBASQUE, Basque Foundation for Science, 48013 Bilbao, Spain²¹Indian Institute of Science Education and Research Mohali, SAS Nagar, 140306, India²²Indian Institute of Technology Bhubaneswar, Satya Nagar 751007, India²³Indian Institute of Technology Guwahati, Assam 781039, India²⁴Indian Institute of Technology Hyderabad, Telangana 502285, India

- ²⁵Indian Institute of Technology Madras, Chennai 600036, India
²⁶Indiana University, Bloomington, Indiana 47408, USA
²⁷Institute of High Energy Physics, Chinese Academy of Sciences, Beijing 100049, China
²⁸Institute of High Energy Physics, Vienna 1050, Austria
²⁹Institute for High Energy Physics, Protvino 142281, Russia
³⁰INFN - Sezione di Napoli, I-80126 Napoli, Italy
³¹INFN - Sezione di Roma Tre, I-00146 Roma, Italy
³²INFN - Sezione di Torino, I-10125 Torino, Italy
³³Advanced Science Research Center, Japan Atomic Energy Agency, Naka 319-1195, Japan
³⁴J. Stefan Institute, 1000 Ljubljana, Slovenia
³⁵Institut für Experimentelle Teilchenphysik, Karlsruher Institut für Technologie, 76131 Karlsruhe, Germany
³⁶Kavli Institute for the Physics and Mathematics of the Universe (WPI), University of Tokyo, Kashiwa 277-8583, Kashiwa, Japan
³⁷Kennesaw State University, Kennesaw, Georgia 30144, USA
³⁸Kitasato University, Sagami-hara 252-0373, Japan
³⁹Korea Institute of Science and Technology Information, Daejeon 34141, South Korea
⁴⁰Korea University, Seoul 02841, South Korea
⁴¹Kyoto Sangyo University, Kyoto 603-8555, Japan
⁴²Kyungpook National University, Daegu 41566, South Korea
⁴³Université Paris-Saclay, CNRS/IN2P3, IJCLab, 91405 Orsay, France
⁴⁴P.N. Lebedev Physical Institute of the Russian Academy of Sciences, Moscow 119991, Russia
⁴⁵Faculty of Mathematics and Physics, University of Ljubljana, 1000 Ljubljana, Slovenia
⁴⁶Ludwig Maximilians University, 80539 Munich, Germany
⁴⁷Luther College, Decorah, Iowa 52101, USA
⁴⁸Malaviya National Institute of Technology Jaipur, Jaipur 302017, India
⁴⁹Faculty of Chemistry and Chemical Engineering, University of Maribor, 2000 Maribor, Slovenia
⁵⁰Max-Planck-Institut für Physik, 80805 München, Germany
⁵¹School of Physics, University of Melbourne, Victoria 3010, Australia
⁵²University of Mississippi, University, Mississippi 38677, USA
⁵³University of Miyazaki, Miyazaki 889-2192, Japan
⁵⁴Moscow Physical Engineering Institute, Moscow 115409, Russia
⁵⁵Graduate School of Science, Nagoya University, Nagoya 464-8602, Japan
⁵⁶Università di Napoli Federico II, I-80126 Napoli, Italy
⁵⁷Nara Women's University, Nara 630-8506, Japan
⁵⁸National Central University, Chung-li 32054, Taiwan
⁵⁹National United University, Miao Li 36003, Taiwan
⁶⁰Department of Physics, National Taiwan University, Taipei 10617, Taiwan
⁶¹H. Niewodniczanski Institute of Nuclear Physics, Krakow 31-342, Poland
⁶²Nippon Dental University, Niigata 951-8580, Japan
⁶³Niigata University, Niigata 950-2181, Japan
⁶⁴Novosibirsk State University, Novosibirsk 630090, Russia
⁶⁵Osaka City University, Osaka 558-8585, Japan
⁶⁶Pacific Northwest National Laboratory, Richland, Washington 99352, USA
⁶⁷Panjab University, Chandigarh 160014, India
⁶⁸Peking University, Beijing 100871, China
⁶⁹University of Pittsburgh, Pittsburgh, Pennsylvania 15260, USA
⁷⁰Punjab Agricultural University, Ludhiana 141004, India
⁷¹Research Center for Nuclear Physics, Osaka University, Osaka 567-0047, Japan
⁷²Meson Science Laboratory, Cluster for Pioneering Research, RIKEN, Saitama 351-0198, Japan
⁷³Dipartimento di Matematica e Fisica, Università di Roma Tre, I-00146 Roma, Italy
⁷⁴Department of Modern Physics and State Key Laboratory of Particle Detection and Electronics, University of Science and Technology of China, Hefei 230026, China
⁷⁵Seoul National University, Seoul 08826, South Korea
⁷⁶Showa Pharmaceutical University, Tokyo 194-8543, Japan
⁷⁷Soongsil University, Seoul 06978, South Korea
⁷⁸Sungkyunkwan University, Suwon 16419, South Korea
⁷⁹School of Physics, University of Sydney, New South Wales 2006, Australia
⁸⁰Tata Institute of Fundamental Research, Mumbai 400005, India
⁸¹Department of Physics, Technische Universität München, 85748 Garching, Germany

⁸²*Toho University, Funabashi 274-8510, Japan*⁸³*Department of Physics, Tohoku University, Sendai 980-8578, Japan*⁸⁴*Earthquake Research Institute, University of Tokyo, Tokyo 113-0032, Japan*⁸⁵*Department of Physics, University of Tokyo, Tokyo 113-0033, Japan*⁸⁶*Tokyo Institute of Technology, Tokyo 152-8550, Japan*⁸⁷*Tokyo Metropolitan University, Tokyo 192-0397, Japan*⁸⁸*Virginia Polytechnic Institute and State University, Blacksburg, Virginia 24061, USA*⁸⁹*Wayne State University, Detroit, Michigan 48202, USA*⁹⁰*Yamagata University, Yamagata 990-8560, Japan*⁹¹*Yonsei University, Seoul 03722, South Korea*⁹²*Department of Physics, Faculty of Science, University of Tabuk, Tabuk 71451, Saudi Arabia*

(Received 10 October 2021; revised 17 February 2023; accepted 22 May 2023; published 13 July 2023)

This paper presents a search for the rare flavor-changing neutral current process $B^0 \rightarrow K^{*0} \tau^+ \tau^-$ using data taken with the Belle detector at the KEKB asymmetric energy e^+e^- collider. The analysis is based on the entire $\Upsilon(4S)$ resonance data sample of 711 fb^{-1} , corresponding to $772 \times 10^6 B\bar{B}$ pairs. In our search we fully reconstruct the companion B meson produced in the process $e^+e^- \rightarrow \Upsilon(4S) \rightarrow B\bar{B}$ from its hadronic decay modes, and look for the decay $B^0 \rightarrow K^{*0} \tau^+ \tau^-$ in the rest of the event. No evidence for a signal is found. We report an upper limit on the branching fraction $\mathcal{B}(B^0 \rightarrow K^{*0} \tau^+ \tau^-) < 3.1 \times 10^{-3}$ at 90% confidence level. This is the first direct limit on $\mathcal{B}(B^0 \rightarrow K^{*0} \tau^+ \tau^-)$.

DOI: [10.1103/PhysRevD.108.L011102](https://doi.org/10.1103/PhysRevD.108.L011102)

The decay $B^0 \rightarrow K^{*0} \tau^+ \tau^-$ (charge-conjugate processes are implied throughout this paper) is of interest for the testing of lepton flavor universality (LFU) and for searches of physics beyond the Standard Model (SM). This decay is highly suppressed in the SM and can only proceed via a flavor-changing neutral current, with a predicted branching fraction of order $\mathcal{O}(10^{-7})$ [1]. The branching fraction can be enhanced if new physics (NP) effects contribute [2–5]. The flavor-changing neutral current processes such as $B^0 \rightarrow K^{*0} \tau^+ \tau^-$ can provide very powerful tests for the SM and its extensions. In particular, the decay is a third-generation equivalent of the $B^0 \rightarrow K^{*0} \ell^+ \ell^-$ decay, where ℓ is an electron or a muon. Hence, compared with electron and muon modes, the decay is expected to be more sensitive to new physics in a model which has a coupling proportionate to the particle mass [6] or only couples to the third generation [7].

Semileptonic B decay measurements in recent years show significant deviations from SM expectations, for both charged and neutral current transitions. The first type of transition has been measured in the decay $b \rightarrow c \ell \bar{\nu}_\ell$ via $R(D^{(*)}) = [\mathcal{B}(B \rightarrow D^{(*)} \tau^+ \nu_\tau)] / [\mathcal{B}(B \rightarrow D^{(*)} \ell^+ \nu_\ell)]$ by the BABAR [8,9], Belle [10–13] and LHCb [14,15] experiments. While these decays are tree-level processes, which are not very sensitive to NP, the measured results show a

deviation of about three standard deviations, 3σ , from the SM predictions (combined significance) [16]. The neutral current transition $b \rightarrow s \ell^+ \ell^-$ is highly suppressed in the SM and very sensitive to NP. The LFU ratio between muons and electrons in the decay mode $B \rightarrow K^{(*)} \ell^+ \ell^-$ as measured by Belle [17–19] and BABAR [20] are consistent with the SM, while LHCb result [21–23] is 3.1σ lower than the SM prediction. Many theoretical models are introduced to explain these anomalies such as the NP contribution to the Wilson coefficients [3,4] and the leptoquark model [5]. These approaches lead to an enhancement of the $b \rightarrow s \tau^+ \tau^-$ branching fraction up to $1\text{--}5 \times 10^{-4}$, three orders of magnitude larger than the SM predictions. The predicted branching fraction of $B^0 \rightarrow K^{*0} \tau^+ \tau^-$ is larger than that of $B^+ \rightarrow K^+ \tau^+ \tau^-$ as shown in Ref. [3].

The presence of at least two neutrinos in the final state originating from the decays of $\tau^+ \tau^-$ pair make analysis of the decay challenging. To date only a search for the decay $B^+ \rightarrow K^+ \tau^+ \tau^-$ has been conducted by the BABAR Collaboration setting an upper limit $\mathcal{B}(B^+ \rightarrow K^+ \tau^+ \tau^-) < 2.25 \times 10^{-3}$ at 90% confidence level (CL) [24].

In this letter, we present the first search for the rare decay $B^0 \rightarrow K^{*0} \tau^+ \tau^-$. Our analysis is based on the complete data set collected at the c.m. energy equal to the $\Upsilon(4S)$ resonance mass by the Belle detector [25] at the KEKB asymmetric-energy e^+e^- collider [26]. This data sample corresponds to an integrated luminosity of 711 fb^{-1} , containing $772 \times 10^6 B\bar{B}$ pairs. We use a full-reconstruction technique [27] in this analysis where the companion B meson in the process $e^+e^- \rightarrow \Upsilon(4S) \rightarrow B\bar{B}$ is reconstructed in hadronic decay modes, referred to as B_{tag} .

Published by the American Physical Society under the terms of the [Creative Commons Attribution 4.0 International license](https://creativecommons.org/licenses/by/4.0/). Further distribution of this work must maintain attribution to the author(s) and the published article's title, journal citation, and DOI. Funded by SCOAP³.

We then search for the signal B meson, B_{sig} , in the rest of the event not used in the B_{tag} reconstruction.

The Belle detector [25] is a large-solid-angle magnetic spectrometer consisting of a silicon vertex detector (SVD), a 50-layer central drift chamber (CDC), an array of aerogel threshold Cherenkov counters (ACC), a barrel-like arrangement of time-of-flight (TOF) scintillation counters, and an electromagnetic calorimeter comprised of CsI(Tl) crystals (ECL). All these components are located inside a superconducting solenoid coil that provides a 1.5 T magnetic field. An iron flux-return located outside of the coil is instrumented with resistive plate chambers to detect K_L^0 mesons and to identify muons (KLM).

We use Monte Carlo (MC) simulation samples, generated with EvtGen [28], to optimize the signal selection, determine the selection efficiencies, as well as to obtain the signal and background fitting models. The detector response is simulated using GEANT3 [29]. Simulated events are overlaid with random trigger data taken for each run period to reproduce the effect of beam-associated backgrounds. A signal sample containing 50 million $\Upsilon(4S) \rightarrow B^0 \bar{B}^0$ events is generated where one B decays to all possible final states, according to its measured or estimated branching fractions [30], and the other decays via $B^0 \rightarrow K^{*0} \tau^+ \tau^-$, using the model described in Ref. [31]. Background MC samples consist of $B^+ B^-$, $B^0 \bar{B}^0$, and continuum $e^+ e^- \rightarrow q \bar{q}$ ($q = u, d, s, c$), where the size of each sample is six times larger than that of collision data. Rare B meson decay processes such as charmless hadronic, radiative, and electroweak decays are simulated separately in a sample designated *Rare B*. Semileptonic $b \rightarrow u \ell \nu$ decays are simulated in a dedicated $u \ell \nu$ sample. The sizes of the *Rare B* and $u \ell \nu$ samples are 50 and 20 times larger than that of collision data, respectively.

A candidate B_{tag} meson is reconstructed in one of the 489 hadronic decay channel using a hierarchical NeuroBayes-based (NB) full-reconstruction algorithm [27]. In this algorithm, the continuum backgrounds are suppressed by employed event shape variables such as the polar angle of B_{tag} , the cosine of the angle between the thrust axis [32] and z -direction, and the modified second Fox-Wolfram moment [33]. All the input variables which used during the reconstruction are mapped to a single classifier output, \mathcal{O}_{NB} , which represents the quality of B_{tag} , ranges from zero for combinatorial background and continuum events to unity for an unambiguous B_{tag} . Event selection also exploits the energy difference $\Delta E = E_{B_{\text{tag}}} - E_{\text{cm}}/2$ and the beam-energy-constrained mass $M_{\text{bc}} = \sqrt{(E_{\text{cm}}/2)^2/c^4 - |\vec{p}_{B_{\text{tag}}}|^2/c^2}$, where E_{cm} is the $e^+ e^-$ energy, and $E_{B_{\text{tag}}}$ and $\vec{p}_{B_{\text{tag}}}$ are the reconstructed energy and momentum of the B_{tag} candidate, respectively. All the quantities are measured in the c.m. frame. We require each B_{tag} candidate to satisfy $\ln(\mathcal{O}_{\text{NB}}) > -7$, $|\Delta E| < 0.06$ GeV, and $5.275 < M_{\text{bc}} < 5.290$ GeV/ c^2 .

The net tagging efficiency which is defined as number of truly reconstructed B -tag divided for total number of generated event is 0.24%. It is slightly higher than that reported in Ref. [27], due to lower average particle multiplicity in this signal sample compared to generic sample. The signal side of the $B^0 \rightarrow K^{*0} \tau^- \tau^+$ sample contains of leptons and only two hadron tracks. The possibility of the interference from signal side to the tag side reconstruction is lower than that of the generic samples, where both B mesons decay generically. The tagging efficiency is calibrated by comparing the known branching fraction from PDG [30] of the decays $B \rightarrow D^{(*)} \ell \nu_\ell$ and the measured values which use this hadron tag reconstruction method [34].

For events where a B_{tag} is reconstructed, we search for the decay $B^0 \rightarrow K^{*0} \tau^+ \tau^-$ in the rest of the event. The remaining tracks are examined to remove duplicate ones due to the curling of low transverse-momentum particles ($p_t < 0.3$ GeV/ c). A pair of tracks is considered as duplicate if the cosine of the angle between them is either larger than 0.9 or smaller than 0.1, and the difference in transverse momentum is less than 0.1 GeV/ c . All tracks are constrained to originate from the interaction point (IP) by the requirements $|dr| < 2$ cm and $|dz| < 4$ cm, where dr and dz are the impact parameter with respect to IP in the transverse and longitudinal directions, respectively. We select events as signal candidates if there are four remaining tracks with zero net charge. The number of signal candidates doubles after removing duplicate tracks.

We reconstruct candidate K^{*0} mesons from $K^{*0} \rightarrow K^+ \pi^-$ decays using two of the four remaining tracks. We identify kaons and pions based on combined information from the CDC, ACC, and TOF [35]. A charged track is identified as a kaon if the likelihood ratio $\mathcal{R}_K = \mathcal{L}_K / (\mathcal{L}_K + \mathcal{L}_\pi) > 0.6$, and as a pion if $\mathcal{R}_K < 0.4$, where \mathcal{L}_i is the PID likelihood for the particle type i . The momenta of K^+ and π^- candidates are required to be greater than 0.1 GeV/ c . The flavor of the reconstructed K^{*0} and hence the corresponding flavor of B_{sig} is required to be opposite to that of B_{tag} . This requirement rejects 20% of the events. We fit the vertex for K^{*0} candidates, and reject candidates if the vertex fit fails. If more than one K^{*0} candidate is successfully reconstructed, the one having the reconstructed mass closest to the known K^{*0} mass is retained. We require the mass of the reconstructed K^{*0} candidate to be in the range $[0.8, 1.0]$ GeV/ c^2 , which is approximately twice the decay width of K^{*0} . We consider three τ decay modes in this analysis: $\tau^- \rightarrow e^- \bar{\nu}_e \nu_\tau$, $\tau^- \rightarrow \mu^- \bar{\nu}_\mu \nu_\tau$, and $\tau^- \rightarrow \pi^- \nu_\tau$, resulting in six different decay topologies: $K^{*0} e^+ e^-$, $K^{*0} e^\mp \mu^\pm$, $K^{*0} \mu^+ \mu^-$, $K^{*0} e^\mp \pi^\pm$, $K^{*0} \mu^\mp \pi^\pm$, and $K^{*0} \pi^+ \pi^-$. We regard the two remaining tracks not used in the B_{tag} or the K^{*0} candidates as τ decay products. The reconstructed mass of these two tracks is required to be less than 2.5 GeV/ c^2 .

All the tracks and clusters in a signal event are used for the reconstruction of B_{tag} and B_{sig} . However, there are still tracks and clusters from beam background and possible duplicate tracking reconstruction. We require that there be no extra π^0 nor K_S^0 candidates, and at most one K_L^0 candidate cluster, to allow for beam-associated backgrounds or electronic noise. We reconstruct K_L^0 candidates based on the hit patterns in the KLM subdetector not associated with any charged track. A π^0 candidate is reconstructed from $\pi^0 \rightarrow \gamma\gamma$ in which neither daughter photon is included in the reconstructed B_{tag} and whose reconstructed mass is within $25 \text{ MeV}/c^2$ of the nominal π^0 mass [30], corresponding to 3σ of the π^0 mass resolution. Energy of photon candidates must exceed 50 MeV and we require their shower shape, characterized as the ratio of total energy detected in a 3×3 versus 5×5 array of ECL crystals in which the center crystal has the maximum detected energy, to be larger than 0.75 . We reconstruct candidate K_S^0 from $K_S^0 \rightarrow \pi^+\pi^-$ decays, where the reconstructed mass is within $15 \text{ MeV}/c^2$ of the nominal mass, corresponding to 3σ of K_S^0 mass resolution.

We determine the number of signal candidates by fitting the distribution of extra calorimeter energy, $E_{\text{ECL}}^{\text{extra}}$, which is defined as the total energy of the neutral clusters detected in the ECL not associated with either B_{tag} or B_{sig} . We reduce the contribution of beam-associated backgrounds while estimating $E_{\text{ECL}}^{\text{extra}}$ by only counting clusters with energy greater than 0.15 GeV , 0.05 GeV and 0.10 GeV for the backward, barrel, and forward regions, respectively. In signal events $E_{\text{ECL}}^{\text{extra}}$ should be zero or have a small value due to the residual energy from beam-associated backgrounds or mismatched tracks. Background events tend to have larger values due to contributions from additional neutral clusters. We select events with $E_{\text{ECL}}^{\text{extra}} < 0.2 \text{ GeV}$ as the signal region and those with $E_{\text{ECL}}^{\text{extra}} < 2 \text{ GeV}$ for sideband studies. The selection criteria in this study are chosen to maximize the search sensitivity in the signal region following the Punzi figure of merit [36].

In the c.m. frame, the B_{tag} and B_{sig} have opposite flight directions, and the B_{tag} is fully reconstructed and its four-vector is determined. The momentum of B_{sig} is thus derived from the B_{tag} reconstruction. Its direction is opposite the B_{tag} and its magnitude is calculated as $|\vec{p}_{B_{\text{sig}}}| = \sqrt{(E_{\text{cm}}/2)^2/c^2 - m_B^2}$, where $\vec{p}_{B_{\text{sig}}}$ is the momentum vector of B_{sig} , $E_{\text{cm}}/2$ is the beam energy measured in c.m. frame, and m_B is the nominal B^0 meson mass [30]. We calculate the $\tau^+\tau^-$ pair invariant mass, $M_{\tau^+\tau^-}$, by subtracting the reconstructed K^{*0} c.m. four-vector from the B_{sig} 's giving its kinematic limits. We require $M_{\tau^+\tau^-}$ to be greater than $3.55 \text{ GeV}/c^2$ to suppress combinatorial background.

After the selections above, the remaining background is final-state dependent. We classify the remaining events into signal modes based on final-state particles for further

background suppression. We identify electron candidates using an electron likelihood ratio, $\mathcal{R}_e = \mathcal{L}_e/(\mathcal{L}_e + \mathcal{L}_{\bar{e}})$, \bar{e} indicates nonelectron hypothesis. \mathcal{L}_e ($\mathcal{L}_{\bar{e}}$) are calculated based on dE/dx information from the CDC, the ratio of the energy deposited in the ECL to the momentum measured by the CDC and SVD, the shower shape in the ECL, hit information from the ACC, and matching between the position of the charged track and the ECL cluster [37]. Muon candidates are identified using a muon likelihood ratio, $\mathcal{R}_\mu = \mathcal{L}_\mu/(\mathcal{L}_\mu + \mathcal{L}_\pi + \mathcal{L}_K)$, which is estimated based on the difference between the range of the track in KLM, estimated assuming no hadronic interactions, and the actual range observed in the KLM. A χ^2 from extrapolating a track to the signals identified in the KLM using a Kalman filter also contributes to the likelihood [38]. Tracks are identified as electrons if $\mathcal{R}_e > 0.8$, as muons if not satisfying the electron requirement and have $\mathcal{R}_\mu > 0.8$, and as a pion if not either an electron or a muon. The average of electron (muon) identification efficiency for the selection $\mathcal{R}_{e(\mu)} > 0.8$ is 92 (92)% with pion fake rate of 0.25 (2.5)%. In the signal decay modes $K^{*0}\pi^+\pi^-$ and $K^{*0}\ell^\pm\pi^\mp$, there remains a large background contribution from the decay $B^0 \rightarrow D^{(*)-}\ell^+\nu_\ell$, where $D^{(*)-} \rightarrow K^{*0}\pi^-$ (π^0). We suppress this by requiring the invariant mass $M_{K^{*0}\pi^-}$ to lie outside the D^- mass region, $M_{K^{*0}\pi^-} < 1.84 \text{ GeV}/c^2$ or $M_{K^{*0}\pi^-} > 1.94 \text{ GeV}/c^2$, where $M_{K^{*0}\pi^-}$ is the combination of the K^{*0} candidate and a track that is opposite to the charge of the kaon candidate in the K^{*0} decay. Combinatorial background is also significant in these signal modes, and so the \mathcal{O}_{NB} selection criterion is tightened to $\ln(\mathcal{O}_{\text{NB}}) > -4$ for these modes.

After we apply above selection criteria, our simulation predicts that the remaining backgrounds with low $E_{\text{ECL}}^{\text{extra}}$ are primarily $B^0\bar{B}^0$ events in which a B_{tag} is properly reconstructed opposite $B^0 \rightarrow D^-\ell^+\nu_\ell$ decaying to $D^- \rightarrow K^{*0}\ell^-\bar{\nu}_\ell$. Such events have the same final-state particles as signal events. The different number of missing neutrinos results in a different missing mass distribution, M_{miss} . We calculate this by subtracting the measured part of the four-momentum of B_{sig} from the derived four-momentum of B_{sig} from the recoil against B_{tag} . In addition to the missing mass, we find $M_{K^{*0}\pi^-}$ is also powerful distinguishing signal from the remaining background. For $K^{*0}\ell^-\ell^+$ modes, we calculate $M_{K^{*0}\pi^-}$ by combining the negatively charged lepton with the K^{*0} assuming a pion mass. We optimize selection criteria based on M_{miss}^2 and $M_{K^{*0}\pi^-}$ together mode-by-mode. These are summarized in Table I. Since the number of missing neutrinos from the $K^{*0}\pi^+\pi^-$ mode is the same as that from the $B^0 \rightarrow D^-\ell^+\nu_\ell$ background, the M_{miss}^2 is ineffective in rejecting this background. We only apply the selection $M_{\text{miss}}^2 < 9 \text{ GeV}^2/c^4$ to reject combinatorial background which is significant in this mode. Despite the continuum suppression performed by the full reconstruction algorithm, a small fraction of continuum

TABLE I. Summary of the selection criteria imposed on $M_{K^{*0}\pi^-}$ and M_{miss}^2 for each of the signal modes.

Signal mode	$M_{K^{*0}\pi^-}$ (GeV/ c^2)	M_{miss}^2 (GeV $^2/c^4$)
$K^{*0}e^+e^-$	>1.4	>3.2
$K^{*0}e^\mp\mu^\pm$	>1.4	>1.6
$K^{*0}\mu^+\mu^-$	>1.6	>1.6
$K^{*0}\pi^+e^\pm$	>1.4	>2.0
$K^{*0}\pi^\mp\mu^\pm$	>1.4	>2.0
$K^{*0}\pi^+\pi^-$	>1.5	<9

events remains in the $K^{*0}\pi^+\pi^-$ signal mode. In this case, further constraints on the event shape are imposed. Specifically, the event thrust is required to be smaller than 0.85, the cosine of the angle between the thrust of B_{sig} and that of B_{tag} must be smaller than 0.85, and the modified second Fox-Wolfram moment is required to be less than 0.4.

We estimate the signal reconstruction efficiency after applying all of the selection criteria and B_{tag} efficiency corrections. The overall selection efficiency, determined using simulated $B^0 \rightarrow K^{*0}\tau^+\tau^-$ decays, is approximately $(1.23 \pm 0.05) \times 10^{-5}$, where the uncertainty is statistical. The signal yield is extracted with a binned extended maximum-likelihood fit to the $E_{\text{ECL}}^{\text{extra}}$ distribution, with a bin width of 0.1 GeV. The probability density functions (PDFs) for signal and background components are taken from MC expectations after applying the B-tag efficiency correction. To reduce the uncertainty due to low statistics, a simulation sample three times larger than the data is used to construct the background PDFs, the signal PDF is derived from 50 million $\Upsilon(4S) \rightarrow B^0\bar{B}^0$ signal events, and signal modes are combined in the fit. The B^+B^- and $B^0\bar{B}^0$ samples are normalized to the data and their ratio is fixed in the fit. Contributions from *Rare B* and $u\ell\nu_\ell$ components in the final sample are negligible, and are normalized to the number of $B\bar{B}$ pairs and fixed in the fit. We float the $B\bar{B}$, continuum, and signal normalizations. We have validated the fitting procedure in tests with MC samples.

We test the analysis procedure and shape of the simulated $E_{\text{ECL}}^{\text{extra}}$ distribution using $B^0 \rightarrow D^-\ell^+\nu_\ell$ decays, with $D^- \rightarrow K^{*0}\pi^-$. The analysis steps and selection criteria for the decay are the same as those for the $B^0 \rightarrow K^{*0}\tau^+\tau^-$ decay, except the requirement on M_{miss}^2 is removed and the selection on $M_{K^{*0}\pi^-}$ is reversed, requiring $1.84 < M_{K^{*0}\pi^-} < 1.94$ GeV/ c^2 . We divided the sample into the two sub-samples, one with $M_{\text{miss}}^2 < 0.5$ GeV $^2/c^4$ and the other with $M_{\text{miss}}^2 > 0.5$ GeV $^2/c^4$. The first subsample where events are mainly from $B^0 \rightarrow D^-\ell^+\nu_\ell$ is useful for checking the signal shape. The latter containing mostly background events is used for validate the background shape. Within statistics, the signal and background models obtained from simulation are in good agreement with the data and are used

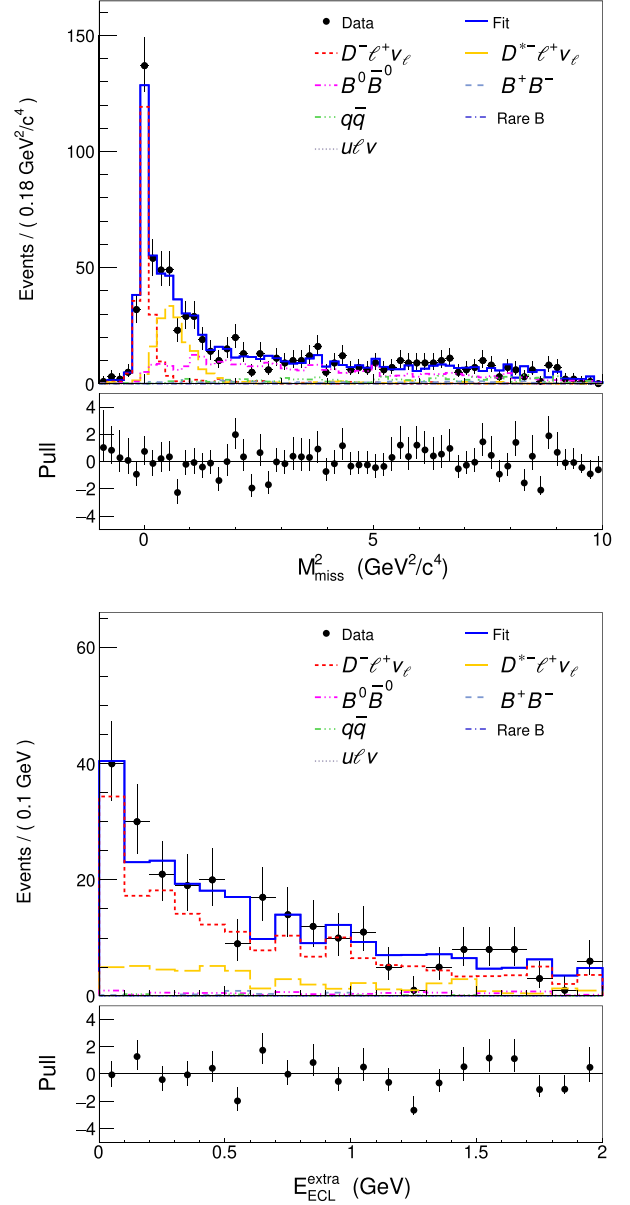


FIG. 1. Fit results for M_{miss}^2 (upper) and $E_{\text{ECL}}^{\text{extra}}$ (lower) for the decays $B^0 \rightarrow D^{(*)}\ell^+\nu_\ell$. The dots with error bars represent the data, and the blue line indicates the fitted results. The dashed lines indicate different fit components. $E_{\text{ECL}}^{\text{extra}}$ is plotted with the selection $M_{\text{miss}}^2 < 0.5$ GeV $^2/c^4$.

to model the signal and background in the final fit. As a cross-check, we measure the branching fraction of the decay $B^0 \rightarrow D^-\ell^+\nu_\ell$ from a fit to the $E_{\text{ECL}}^{\text{extra}}$ distributions, similar to our search for the decay $B^0 \rightarrow K^{*0}\tau^+\tau^-$, and also to the M_{miss}^2 distribution. Results of these fits are shown in Fig. 1. The branching fraction measured by fitting to $E_{\text{ECL}}^{\text{extra}}$ for the first subsample is $(2.45 \pm 0.17)\%$ and to M_{miss}^2 is $(2.37 \pm 0.15)\%$, where the quoted uncertainties are statistical only. The results are in good agreement with the world average of $2.31 \pm 0.10\%$ [30]. We obtained a zero

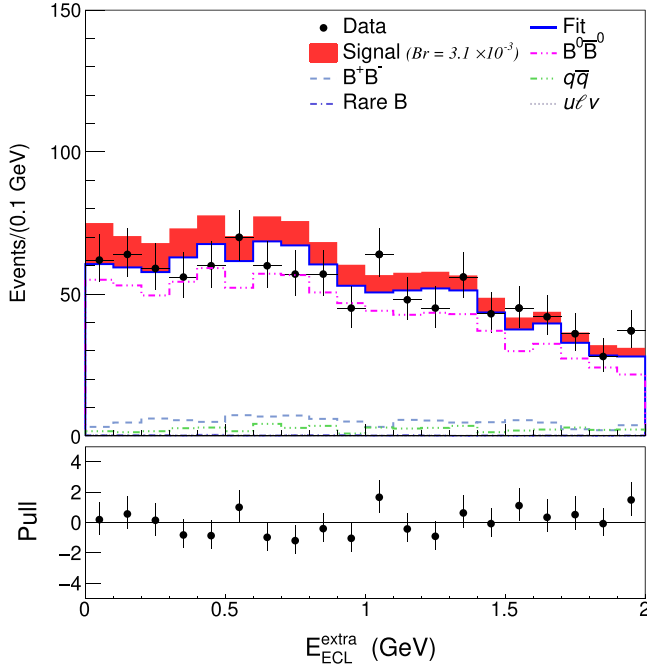


FIG. 2. Distribution of $E_{\text{ECL}}^{\text{extra}}$ combined for all signal modes. The dots with error bars show the data, the blue line shows the fitted results with the background-only model, and the dashed lines show fit results for the different components. A signal (red region) with a branching fraction of 3.1×10^{-3} , corresponding to the upper limit at 90% CL, is superimposed on the top of the fit.

signal for the fit to $E_{\text{ECL}}^{\text{extra}}$ distribution of the second subsample ($M_{\text{miss}}^2 > 0.5 \text{ GeV}^2/c^4$) as expected.

We perform the fit to $E_{\text{ECL}}^{\text{extra}}$ for the decay $B^0 \rightarrow K^{*0} \tau^+ \tau^-$ using the procedure as described above, where all signal modes have been combined. The numbers of signal and background events in the signal window $[0; 0.2] \text{ GeV}$ obtained from the fit are $N_{\text{sig}} = -4.9 \pm 6.0$ and $N_{\text{bkg}} = 122.4 \pm 4.9$, respectively. We find no evidence for a signal. Data are consistent with background as shown in Fig. 2, where the background-only model is fitted to data and a signal with branching fraction of 3.1×10^{-3} is superimposed on the top.

Systematic uncertainties on the number of background events, the signal reconstruction efficiency, and number of $B\bar{B}$ pairs arise from several sources and affect the branching fraction upper limit. The uncertainty on number of $B\bar{B}$ pairs is 1.8%. The statistical uncertainty on the selection efficiency due to limited MC sample size is estimated to be 4.0%. The uncertainty associated with the B_{tag} efficiency is 5.1%, which is estimated using various decays as studied in Ref. [34]. Tracking uncertainty is assigned to be 1.4% for the four B_{sig} charged tracks. The uncertainty due to the charged track selection is estimated to be 4.1%. Particle identification impacts K^{*0} reconstruction and signal mode separation, hence the uncertainties from electron, muon, and pion identification are weighted following their fraction

in the signal mode. The total particle identification uncertainty is 2.55%. The difference in reconstruction efficiency for π^0 and K_S^0 leads to a systematic uncertainty in application of the corresponding vetoes. Their uncertainties are estimated to be 0.17% and 1.56% for π^0 and K_S^0 , respectively. The uncertainty on the branching fraction of τ is 0.57%. The total systematic uncertainty is 8.5% calculated by summing the above uncertainties in quadrature.

The systematic uncertainty due to the statistical error of the PDF templates is estimated by varying bin contents of the templates following the Poisson distribution and repeating the fit to the data. This step is repeated 1000 times for each of the PDF. The standard deviation of the number of signal distribution obtained from the fits is considered as systematics uncertainty. The total uncertainty is 4.59 events.

The signal yield obtained from the extended maximum-likelihood fit is translated into an upper limit on the $B \rightarrow K^{*0} \tau^+ \tau^-$ branching fraction using the CL_s method [39,40]. We account for statistical and systematic uncertainties on the number of background events and signal efficiencies by modeling them as Gaussian functions with standard deviations given by their uncertainties. Our observed upper limit on the $B \rightarrow K^{*0} \tau^+ \tau^-$ branching fraction is 3.1×10^{-3} at 90% CL.

In conclusion, we have performed a search for the decay $B \rightarrow K^{*0} \tau^+ \tau^-$ using the full Belle data set collected at the c.m. energy of the $\Upsilon(4S)$ resonance. We find no signal and set an upper limit on the branching fraction to be 3.1×10^{-3} at 90% CL. This is the first experimental limit on the decay $B \rightarrow K^{*0} \tau^+ \tau^-$.

ACKNOWLEDGMENTS

We thank the KEKB group for the excellent operation of the accelerator; the KEK cryogenics group for the efficient operation of the solenoid; and the KEK computer group, and the Pacific Northwest National Laboratory (PNNL) Environmental Molecular Sciences Laboratory (EMSL) computing group for strong computing support; and the National Institute of Informatics, and Science Information NETwork 5 (SINET5) for valuable network support. We acknowledge support from the Ministry of Education, Culture, Sports, Science, and Technology (MEXT) of Japan, the Japan Society for the Promotion of Science (JSPS), and the Tau-Lepton Physics Research Center of Nagoya University; the Australian Research Council including Grants No. DP180102629, No. DP170102389, No. DP170102204, No. DP150103061, and No. FT130100303; Austrian Federal Ministry of Education, Science and Research (FWF) and FWF Austrian Science Fund No. P 31361-N36; the National Natural Science Foundation of China under Contracts No. 11435013, No. 11475187, No. 11521505, No. 11575017, No. 11675166, and No. 11705209; Key Research Program of Frontier Sciences, Chinese Academy

of Sciences (CAS), Grant No. QYZDJ-SSW-SLH011; the CAS Center for Excellence in Particle Physics (CCEPP); the Shanghai Science and Technology Committee (STCSM) under Grant No. 19ZR1403000; the Ministry of Education, Youth and Sports of the Czech Republic under Contract No. LTT17020; Horizon 2020 ERC Advanced Grant No. 884719 and ERC Starting Grant No. 947006 “InterLeptons” (European Union); the Carl Zeiss Foundation, the Deutsche Forschungsgemeinschaft, the Excellence Cluster Universe, and the VolkswagenStiftung; the Department of Atomic Energy (Project Identification No. RTI 4002) and the Department of Science and Technology of India; the Istituto Nazionale di Fisica Nucleare of Italy; National Research Foundation (NRF) of Korea Grants No. 2016R1D1A1B01010135, No. 2016R1D1A1B02012900, No. 2018R1A2B3003643, No. 2018R1A6A1A06024970, No. 2019K1A3A7A09033840, No. 2019R1I1A3A01058933, No. 2021R1A6A1A03043957,

No. 2021R1F1A1060423, and No. 2021R1F1A1064008; Radiation Science Research Institute, Foreign Large-size Research Facility Application Supporting project, the Global Science Experimental Data Hub Center of the Korea Institute of Science and Technology Information and KREONET/GLORIAD; the Polish Ministry of Science and Higher Education and the National Science Center; the Ministry of Science and Higher Education of the Russian Federation, Agreement No. 14.W03.31.0026, and the HSE University Basic Research Program, Moscow; University of Tabuk research Grants No. S-1440-0321, No. S-0256-1438, and No. S-0280-1439 (Saudi Arabia); the Slovenian Research Agency Grants No. J1-9124 and No. P1-0135; Ikerbasque, Basque Foundation for Science, Spain; the Swiss National Science Foundation; the Ministry of Education and the Ministry of Science and Technology of Taiwan; and the United States Department of Energy and the National Science Foundation.

-
- [1] J. L. Hewett, *Phys. Rev. D* **53**, 4964 (1996).
 - [2] J. F. Kamenik, S. Monteil, A. Semkiv, and L. Vale Silva, *Eur. Phys. J. C* **77**, 701 (2017).
 - [3] B. Capdevila, A. Crivellin, S. Descotes-Genon, L. Hofer, and J. Matias, *Phys. Rev. Lett.* **120**, 181802 (2018).
 - [4] R. Alonso, B. Grinstein, and J. Martin Camalich, *J. High Energy Phys.* **10** (2015) 184.
 - [5] A. Crivellin, D. Müller, and T. Ota, *J. High Energy Phys.* **09** (2017) 040.
 - [6] E. O. Iltan, G. Turan, and I. Turan, *J. Phys. G* **28**, 307 (2002).
 - [7] L. Calibbi, A. Crivellin, and T. Ota, *Phys. Rev. Lett.* **115**, 181801 (2015).
 - [8] J. P. Lees *et al.* (BABAR Collaboration), *Phys. Rev. Lett.* **109**, 101802 (2012).
 - [9] J. P. Lees *et al.* (BABAR Collaboration), *Phys. Rev. D* **88**, 072012 (2013).
 - [10] M. Huschle *et al.* (Belle Collaboration), *Phys. Rev. D* **92**, 072014 (2015).
 - [11] Y. Sato *et al.* (Belle Collaboration), *Phys. Rev. D* **94**, 072007 (2016).
 - [12] S. Hirose *et al.* (Belle Collaboration), *Phys. Rev. Lett.* **118**, 211801 (2017).
 - [13] G. Caria *et al.* (Belle Collaboration), *Phys. Rev. Lett.* **124**, 161803 (2020).
 - [14] R. Aaij *et al.* (LHCb Collaboration), *Phys. Rev. Lett.* **115**, 111803 (2015).
 - [15] R. Aaij *et al.* (LHCb Collaboration), *Phys. Rev. Lett.* **120**, 171802 (2018).
 - [16] Y. S. Amhis *et al.* (Heavy Flavor Averaging Group), *Eur. Phys. J. C* **81**, 226 (2021).
 - [17] J.-T. Wei *et al.* (Belle Collaboration), *Phys. Rev. Lett.* **103**, 171801 (2009).
 - [18] S. Wehle *et al.* (Belle Collaboration), *Phys. Rev. Lett.* **126**, 161801 (2021).
 - [19] S. Wehle *et al.* (Belle Collaboration), *Phys. Rev. Lett.* **118**, 111801 (2017).
 - [20] J. P. Lees *et al.* (BABAR Collaboration), *Phys. Rev. D* **86**, 032012 (2012).
 - [21] R. Aaij *et al.* (LHCb Collaboration), *Phys. Rev. Lett.* **113**, 151601 (2014).
 - [22] R. Aaij *et al.* (LHCb Collaboration), *J. High Energy Phys.* **2017** 08, 055.
 - [23] R. Aaij *et al.* (LHCb Collaboration), *Nat. Phys.* **18**, 277 (2022).
 - [24] J. P. Lees *et al.* (BABAR Collaboration), *Phys. Rev. Lett.* **118**, 031802 (2017).
 - [25] A. Abashian *et al.*, *Nucl. Instrum. Methods Phys. Res., Sect. A* **479**, 117 (2002), also see Section 2 in J. Brodzicka *et al.*, *Prog. Theor. Exp. Phys.* **2012**, 04D001 (2012).
 - [26] S. Kurokawa and E. Kikutani, *Nucl. Instrum. Methods Phys. Res., Sect. A* **499**, 1 (2003), and other papers included in this Volume; T. Abe *et al.*, *Prog. Theor. Exp. Phys.* **2013**, 03A001 (2013) and references therein.
 - [27] M. Feindt, F. Keller, M. Kreps, T. Kuhr, S. Neubauer, D. Zander, and A. Zupanc, *Nucl. Instrum. Methods Phys. Res., Sect. A* **654**, 432 (2011).
 - [28] D. J. Lange, *Nucl. Instrum. Methods Phys. Res., Sect. A* **462**, 152 (2001), BEAUTY2000, Proceedings of the 7th Int. Conf. on B-Physics at Hadron Machines.
 - [29] R. Brun *et al.*, CERN Report No. CERN-DD-EE-84-1, 1987.
 - [30] P. A. Zyla *et al.* (Particle Data Group), *Prog. Theor. Exp. Phys.* **2020**, 083C01 (2020).
 - [31] A. Ali, E. Lunghi, C. Greub, and G. Hiller, *Phys. Rev. D* **66**, 034002 (2002).

- [32] S. Brandt *et al.*, *Phys. Lett.* **12**, 57 (1964).
- [33] G.C. Fox and S. Wolfram, *Phys. Rev. Lett.* **41**, 1581 (1978).
- [34] A. Sibidanov *et al.* (Belle Collaboration), *Phys. Rev. D* **88**, 032005 (2013).
- [35] E. Nakano, *Nucl. Instrum. Methods Phys. Res., Sect. A* **494**, 402 (2002).
- [36] G. Punzi, eConf C **030908**, MODT002 (2003).
- [37] K. Hanagaki, H. Kakuno, H. Ikeda, T. Iijima, and T. Tsukamoto, *Nucl. Instrum. Methods Phys. Res., Sect. A* **485**, 490 (2002).
- [38] A. Abashian *et al.*, *Nucl. Instrum. Methods Phys. Res., Sect. A* **491**, 69 (2002).
- [39] A.L. Read, *J. Phys. G* **28**, 2693 (2002).
- [40] G. Cowan, K. Cranmer, E. Gross, and O. Vitells, *Eur. Phys. J. C* **71**, 1554 (2011); **73**, 2501(E) (2013).